Available online at www.sciencedirect.com
SCIENCE DIRECT®
International Journal of Multiphase Flow 29 (2003) 1669–1683
International Journal of Multiphase Flow
www.elsevier.com/locate/ijmulflow

Direct steam generation in parallel pipes

Sivan Natan, Dvora Barnea, Yehuda Taitel *

Department of Fluid Mechanics and Heat Transfer, Faculty of Engineering, Tel-Aviv University, Ramat-Aviv 69978, Israel

Received 17 July 2002; received in revised form 17 July 2003

Abstract

Two-phase flow in parallel pipes is associated with the application of direct steam generation (DSG) by solar heating using parabolic troughs focusing solar power. In this process water is fed into parallel pipes from a common manifold. Owing to local cloud cover or difference in the focusing quality, each pipe may receive a different heating power. In this case the flow rate in each pipe will be different.

It is the purpose of this work to analyze a system of two parallel pipes with common inlet and outlet manifolds. Subcooled water that enters the system undergoes a process of heating and evaporation. The results show that the solution is not unique and one can obtain 1, 3 or 5 solutions, even for the case of equal heating of the two pipes. Each solution yields the flow rate in each pipe and the distribution of temperature, pressure, quality and holdup along the pipes.

It was found that for most cases, the water tend to flow in the pipe which absorb less heat. This is an unfavorable conclusion from the practical operational point of view.

1. Introduction

Direct steam generation (DSG) by solar heating, using parabolic troughs focussing solar power on long pipes involves a process of two phase flow in the pipes that undergoes an evaporation process. In this process subcooled water is fed into many parallel pipes from a common manifold. The desired operation is that all pipes will receive the same power of heat input and that the flow conditions in each pipe are the same. This may not be the case in practice. Owing to local cloud cover or differences in focusing quality, each pipe may receive a different heating power. In this case the flow rate in each pipe is different.

* Corresponding author. Tel.: +972-3-640-8220; fax: +972-3-640-7334.
E-mail address: taitel@eng.tau.ac.il (Y. Taitel).

0301-9322/$ - see front matter © 2003 Elsevier Ltd. All rights reserved.
doi:10.1016/j.ijmultiphaseflow.2003.07.002

Jovic et al. (1994) investigated experimentally the onset of pressure drop oscillations in two phase air water flow in three parallel channels. The fluids were fed separately to each pipe while the exit was common. It was shown that unstable flow can take place.

Ozawa et al. (1979, 1982, 1989) studied experimentally two-phase flow in capillary parallel pipes of 3.1 mm diameter. They attempted to simulate flow in boiling channels by the injection of air and water along the pipes. Their conclusion is that the injection of air has a destabilizing effect on the pressure drop oscillations. On the other hand, the injection of liquid has a stabilizing effect, but induces a small-amplitude oscillation in the liquid flow rates.

The work of Reinecke et al. (1994) focuses on flow reversal in vertical two-phase flow in parallel channels that is related to loss of coolant accident (LOCA) or to loss of pumping power accident (LOPP) in nuclear plants. Their experimental set up consists of six tubes with an inner diameter of 19.05 mm and a length of 1.3 m connecting a top and a bottom plenum. The two-phase mixture was fed into the bottom plenum and experiments were carried out to determine the boundaries of the reversal state. A model, based on pressure drop calculations was presented for the prediction of the reversal boundaries. The boundaries for reversal two-phase flow in a multiple tube array are determined when the hydrostatic pressure drop exceeds the system pressure.

Tshuva et al. (1999) investigated the splitting of adiabatic two-phase flow in a system of two parallel pipes with a common feed and a common exit. They mapped experimentally the conditions of even and uneven splitting of the two phases in the pipes. The results show that at low flow rates and in inclined pipes the flow is not symmetric. The experimental results are compared with a theoretical model.

It is the purpose of this work to analyze a system of two parallel pipes in which water undergoes heating and evaporation. A numerical simulation is developed capable of calculating the splitting of the flow between the two pipes, and the properties of the fluids along the pipes.

2. Analysis

Fig. 1 shows schematically the geometry involved. Two pipes are placed in parallel and have a common input manifold and a common output manifold. Subcooled water enters the input manifold and the flow splits into the two heated parallel pipes.

Heating and evaporation is taking place in the two pipes. water can exit the outlet as hot liquid, liquid–vapor mixture or superheated vapor, depending on the flow rate and heating power. It is assumed that the liquid input W_{in} is known, the pressure at the outlet is set and the impinging

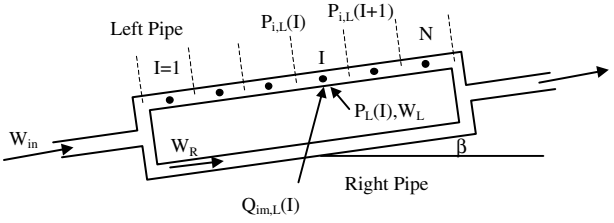

Fig. 1. Schematic flow configuration.

heating along the pipes, Q_{im}, is prescribed. The pressure drop for the two parallel pipes should be the same since they have a common inlet and outlet. Our main objective is to calculate the splitting characteristics of the flow rates and the exit conditions.

2.1. Single pipe analysis

The first step of the analysis considers a single pipe with a given input flow rate and outlet pressure. The pipe is subdivided into N elements. Energy and momentum balances performed on each element allows the calculation of the outlet conditions based on the inlet conditions for each element. Consider an element (I) in which evaporation is taking place, as shown in Fig. 2. At the inlet to element (I) properties such as quality $X_i(I)$, pressure $P_i(I)$, enthalpy $H_i(I)$ and mass flow rate W are considered known. The exit pressure of element (I) (the inlet pressure of element $(I+1)$), $P_i(I+1)$, is initially assumed by linear extrapolation of the pressure upstream. Then the pressure of the element is calculated by

$$P(I) = 0.5(P_i(I) + P_i(I+1)) \tag{1}$$

The heat flow rate per unit length impinging on the pipe wall is considered known and it is designated as $Q_{im}(I)$ while the amount of heat absorbed by the element is $Q(I)$. Two cases are considered: a case where $Q(I)$ equals $Q_{im}(I)$ and a case where $Q(I)$ has to be calculated using heat transfer model (described in Section 2.3). In this case $Q(I)$ is calculated as a function of $Q_{im}(I)$ and $T(I)$. Note that $T(I)$ is the thermodynamic equilibrium temperature at the pressure $P(I)$. The enthalpy at the exit of the element is calculated by

$$H_i(I+1) = \frac{Q(I) + W \times H_i(I)}{W} \tag{2}$$

The enthalpy of the element is taken as the average between inlet and outlet, namely

$$H(I) = 0.5(H_i(I) + H_i(I+1)) \tag{3}$$

For known pressure and enthalpy of the element all the thermodynamic properties such the quality $X(I)$, the gas and liquid densities $\rho_G(I)$ and $\rho_L(I)$ are defined.

The superficial local flow rates (U_{GS} for the gas and U_{LS} for the liquid) at element I are calculated by

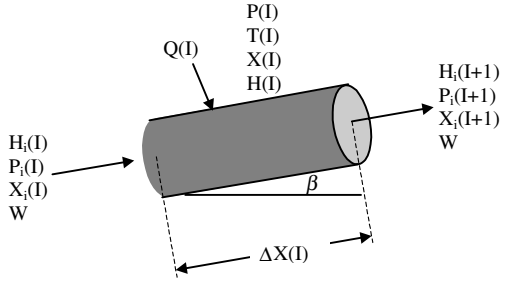

Fig. 2. Heat and momentum balances on a pipe element.

$$U_{GS}(I) = \frac{X(I)W}{A\rho_G(I)} \tag{4}$$

$$U_{LS}(I) = \frac{[1 - X(I)]W}{A\rho_L(I)} \tag{5}$$

where A is the cross-sectional area of the pipe.

Based on the superficial velocities and the gas and liquid properties the pressure drop for each element is calculated (as detailed in Section 2.2) yielding a new value for $P_i(I+1)$. At this point iteration is repeated by going back to Eq. (1) until convergence is reached for the pressure, $P_i(I+1)$.

Note that the aforementioned procedure is valid for the case of gas–liquid mixture, namely, $0 < X < 1$. For subcooled liquid, $X < 0$, or superheated gas, $X > 1$, the procedure is somewhat different. Since the temperature for a single phase is not a function of the pressure only. Thus, the temperature is obtained by an additional internal iteration. $T(I)$ is assumed, $Q(I)$ is evaluated (Section 2.3), then $H_i(I+1)$ and $H(I)$ are evaluated by (2) and (3). $H(I)$ and $P(I)$ yield the new temperature $T(I)$, etc., until convergence is obtained on the value of the temperature.

Once pressure, temperature and flow rate at the pipe inlet are known, the aforementioned procedure allows to calculate the hydrodynamic parameters and properties along the pipe and the pressure at the pipe exit. However, in this work, we consider the exit pressure as an input, thus, this process is followed by an "external" iteration by which the conditions at the pipe inlet are adjusted to satisfy a given pressure at the exit of the pipe.

2.2. Pressure drop

Two methods for the pressure drop calculations are used: (1) A simplified method based on the drift flux model and (2) pressure drop calculation that is based on flow pattern models. In the lather method, the flow pattern is determined according to the local values of the gas and liquid flow rates (Eqs. (4) and (5)). The pressure drop is then calculated based on models related to the particular flow pattern. Taitel and Dukler (1976), Barnea (1987) and Taitel and Barnea (1990) were used for this purpose. Method (2) is too detailed to be presented here. Method (1) however is quite simple and we choose to present it here using drift parameters that correspond to slug flow.

The velocity of the elongated bubbles, U_G, using the drift flux model is

$$U_G = CU_M + U_d \tag{6}$$

where U_M is the mixture velocity which is equal to the sum of the superficial velocities of gas and liquid in the pipe, $U_M = U_{GS} + U_{LS}$. C is the distribution parameter taken as 1.2 for turbulent flow Nicklin (1962) and U_d is the drift velocity, which is the velocity of an elongated bubble in stagnant liquid. U_d, is estimated using Bendiksen (1984) proposal,

$$U_d = 0.54\sqrt{gD}\cos\beta + 0.35\sqrt{gD}\sin\beta \tag{7}$$

where D is the pipe diameter and β is the inclination angle. The average void fraction, α, is

$$\alpha = \frac{U_{GS}}{C(U_{LS} + U_{GS}) + U_d} \tag{8}$$

The pressure drop, ΔP, along each element is calculated as follows:

$$\Delta P = \frac{2}{D} f \rho (U_{LS} + U_{GS})^2 \Delta x + \rho g \sin \beta \Delta x \tag{9}$$

where Δx is the length of an element and ρ is the average density:

$$\rho = \alpha \rho_G + (1 - \alpha)\rho_L \tag{10}$$

The friction factor, f, is calculated using Blasius correlation, $f = cRe^{-n}$, where the Reynolds number Re is given by

$$Re = \frac{(U_{LS} + U_{GS})D\rho}{\mu} \tag{11}$$

$c = 0.046$, $n = 0.2$ for turbulent flow and $c = 16$, $n = 1$ for laminar flow. The viscosity is taken as a weighted average based on the void fraction.

$$\mu = \alpha \mu_G + (1 - \alpha)\mu_L \tag{12}$$

2.3. Heat transfer

Two cases are considered for examining the effect of heating on the flow. In case (1) the heat absorbed by the water is prescribed, that is $Q(I) = Q_{im}(I)$. In case (2) the heat absorbed by the water, $Q(I)$, is calculated via a model that simulates the DSG process.

In the DSG process using solar heating, the water flows in a steel pipe. The steel pipe is placed at the center of a glass pipe. Vacuum in the glass pipe minimizes heat losses to the surroundings. The heat balance for the calculation of $Q(I)$ is formulated using an electrical analog (see Fig. 3). The radiant heat is absorbed by the steel pipe, which is assumed black, and is transferred to the water by conduction and convection via the resistances R_4 and R_5. At the same time heat is lost to the surroundings by convection and radiation via the resistances R_1, R_2 and R_3. Conventional correlations are used for the convective heat transfer coefficients for water and air. The amount of heat absorbed by the water in a pipe element, $Q(I)$, for a given radiant heat flux impinging on a pipe, $Q_{im}(I)$, depends on the temperature of the water, $T(I)$. The heat balance calculation that follows is performed for each element. For simplicity the index (I) is omitted.

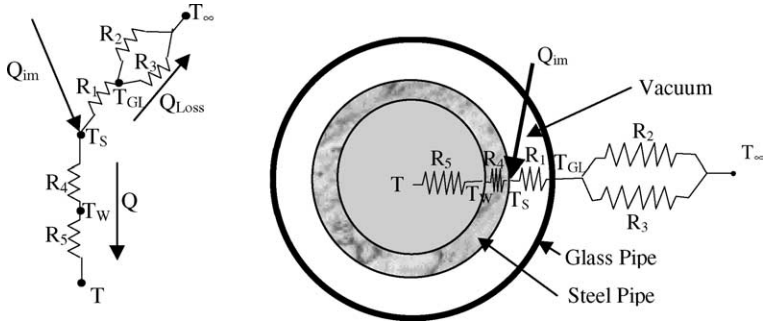

Fig. 3. The heat transfer scheme.

Heat balance on the steel pipe surface yields

$$Q_{\text{im}} = \frac{T_{\text{S}} - T_{\infty}}{R_{123}} + \frac{T_{\text{S}} - T}{R_{45}} \tag{13}$$

where R_{45} is the equivalent resistance of R_4 and R_5. R_{123} is the equivalent resistance of R_1, R_2 and R_3. T_{∞} is the temperature of the surrounding. This equation is used to calculate the steel surface temperature, T_{S}. If the system is in the two-phase state then the water temperature T is a function of the pressure. If the system is in single phase, subcooled liquid or superheated vapor, T is evaluated as a function of the enthalpy and pressure. The temperature T is obtained as part of the iteration process on the pressure drop. Once the temperature T_{S} is calculated, the net heat transported to the water is

$$Q = Q_{\text{im}} - \frac{T_{\text{S}} - T_{\infty}}{R_{123}} \tag{14}$$

For the calculation of the various resistances the following equations are used:

$$\frac{T_{\text{S}} - T_{\text{GL}}}{R_1} = Q_1 = A_{\text{S}} \frac{\sigma \cdot (T_{\text{S}}^4 - T_{\text{GL}}^4)}{\frac{1}{\varepsilon_{\text{S}}} + \frac{A_{\text{S}}}{A_{\text{GL}}}\left(\frac{1}{\varepsilon_{\text{GL}}} - 1\right)} = \left[\frac{A_{\text{S}} \cdot \sigma \cdot (T_{\text{S}}^2 + T_{\text{GL}}^2)(T_{\text{S}} + T_{\text{GL}})}{\frac{1}{\varepsilon_{\text{S}}} + \frac{A_{\text{S}}}{A_{\text{GL}}}\left(\frac{1}{\varepsilon_{\text{GL}}} - 1\right)}\right](T_{\text{S}} - T_{\text{GL}}) \tag{15}$$

where A_{S} is the steel pipe surface area, A_{GL} is the glass pipe surface area and T_{GL} is its temperature, ε_{S} and ε_{GL} are the long wave emissivity coefficients of the steel pipe and the glass pipe and Q_1 is the radiant heat transfer from the steel pipe surface to the glass pipe.

$$\frac{T_{\text{GL}} - T_{\infty}}{R_2} = Q_2 = [\varepsilon_{\text{GL}} \cdot A_{\text{GL}} \cdot \sigma \cdot (T_{\text{GL}}^2 + T_{\infty}^2)(T_{\text{GL}} + T_{\infty})](T_{\text{GL}} - T_{\infty}) \tag{16}$$

Q_2 is the radiant heat transfer from the glass pipe to the surrounding.

$$\frac{T_{\text{GL}} - T_{\infty}}{R_3} = Q_3 = hA_{\text{GL}}(T_{\text{GL}} - T_{\infty}) \quad \text{where } h = 0.237\frac{(T_{\text{GL}} - T_{\infty})^{1/4}}{D_{\text{GL}}} \tag{17}$$

D_{GL} is the glass pipe diameter, h is the free convection heat transfer coefficient and Q_3 is the convective heat transfer from the glass pipe to the surrounding.

$$\frac{T_{\text{S}} - T_{\text{W}}}{R_4} = Q_4 = \frac{T_{\text{S}} - T_{\text{W}}}{\frac{\ln[(D+2\delta)/D]}{2\pi k_{\text{S}} \cdot \Delta x}} \tag{18}$$

k_{S} is the heat conduction of the steel pipe, δ is the pipe wall thickness and Q_4 is the conductive heat transfer through the pipe wall.

$$\frac{T_{\text{W}} - T}{R_5} = Q_5 = h_{\text{TP}} A_{\text{W}}(T_{\text{W}} - T) \tag{19}$$

Q_5 is the convective heat transfer between the inner pipe wall to the water and h_{TP} is the boiling heat convection coefficient given by Tong (1975)

$$\frac{h_{\text{TP}}}{h_{\text{LP}}} = B\left(\frac{1}{X_{\text{tt}}}\right)^n \tag{20}$$

where $B = 2.17$ and $n = 0.7$. For the liquid phase heat transfer coefficient, h_{LP} we use

$$h_{LP} = 0.023 \frac{k_L}{D} \left[\frac{DW(1-X)}{\mu_L} \right]^{0.8} \left(\frac{C_{PL}\mu_L}{k_L} \right)^{0.4} \tag{21}$$

the Lockhart Martinelli parameter for turbulent flow, X_{tt}, is

$$\frac{1}{X_{tt}} = \left(\frac{X}{1-X} \right)^{0.9} \left(\frac{\rho_L}{\rho_G} \right)^{0.5} \left(\frac{\mu_G}{\mu_L} \right)^{0.1}. \tag{22}$$

2.4. Two parallel pipes analysis

The single pipe analysis allows to plot the calculated inlet pressure (for a given outlet pressure) as a function of the flow rate. Such a schematic plot is presented in Fig. 4. The solid line represents the inlet pressure for the right pipe as a function of the flow rate in this pipe for a given heat flux, $Q_{im,R}$. The dashed line presents the inlet pressure vs. flow rate for the left heated pipe, $Q_{im,L}$. In this presentation the heat input for the left pipe is less than for the right pipe.

Since the two pipes are fed from a common manifold, and the fluids exit the system via a common manifold, a solution requires that the pressure drop for the two pipes is the same. It can be seem from Fig. 4 that for a given inlet pressure (given pressure drop) we may have 3 possible flow rates for the right pipe (W_{R1}, W_{R2} and W_{R3}) as well as 3 for the left pipe (W_{L1}, W_{L2} and W_{L3}). Thus 9 steady state solutions for the total inlet flow rate at this particular pressure are possible, namely

$$W_{in} = W_{Ri} + W_{Lj} \quad i = 1 \ldots 3, \;\; j = 1 \ldots 3 \tag{23}$$

Scanning pressure from low to high inlet pressures yields all possible solutions for the pressure drop and the splitting ratio (W_{Ri}/W_{in}) as a function of the total flow rate, W_{in}.

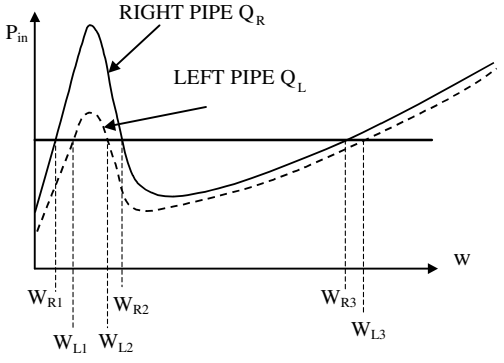

Fig. 4. Schematic inlet pressure variation for the two pipes.

3. Results

Results of the calculations are demonstrated for the following system: The fluid is water, inlet temperature 25 °C, exit pressure 3 MPa, pipe length 400 m, pipe diameter 2.5 cm, inclination angle 10°. Four cases were considered:

(1) Constant heating rate, $Q = Q_{\text{im}}$, pressure drop calculated using the "drift flux" model.
(2) Constant heating rate, $Q = Q_{\text{im}}$, pressure drop calculated using flow pattern models.
(3) Solar heating (Section 2.3), pressure drop calculated using the "drift flux" model.
(4) Solar heating, pressure drop calculated using flow pattern models.

Obviously only limited typical results will be reported here.

3.1. Single pipe

The numerical simulations yield results for the distribution of P, Q, T, X and the flow patterns along the pipe. An example for $W = 0.12$ kg/s and solar heating $Q_{\text{im}} = 1000$ W/m is shown in Fig. 5. Near the pipe entrance the water temperature increases quite fast. Once evaporation starts, the temperature decreases slightly owing to the decrease of the pressure along the pipe. Near the pipe exit the temperature increases again when evaporation is completed and the water is in the form of superheated steam. The pressure decreases monotonically, as expected. Quality increases linearly from 0 to 1 in the range of evaporation. The heat absorbed by the water is maximal when the water is cold, near the entrance. It increases slightly, along the pipe, in the evaporation region owing to the decrease of the temperature along the pipe in this region. The heat absorbed drops drastically in the superheated region, when the steam temperature increases.

Fig. 6 shows the inlet pressure vs. flow rate for 3 typical solar heating. At low flow rates the water evaporates completely near the entrance and the P vs. W curve resemble single-phase steam flow. For high flow rates the behavior is typical of single-phase liquid water flow. For intermediate flow rates, evaporation takes place resulting in a decrease of the pressure drop with flow rate. Note that for the case of $Q = 0$ the typical single-phase water curve is obtained. Fig. 6 is used to generate the solutions for the two pipe system as previously explained.

3.2. Two parallel pipes

Fig. 7 presents the results for the splitting ratio (the ratio of the mass flow rate in the right pipe to the total mass flow rate, $W_{\text{R}}/W_{\text{in}}$) and the inlet pressure vs. the total input flow rate for a symmetric heating. As can be seen the differences between the four cases are relatively small demonstrating that the drift flux model is a reasonable approximation for the solution of this problem. The surprising result is that although the heating is symmetric the solutions may not be symmetric. In fact one can observe regions where 1, 3 or 5 solutions may be obtained for any given value of the input flow rate, W_{in}. A symmetric solution, where the flow rate is the same for both pipes, is a unique solution only for low flow rates and for high flow rates. Note that the flow rate in the left pipe is the complementary to the flow rate in the right pipe.

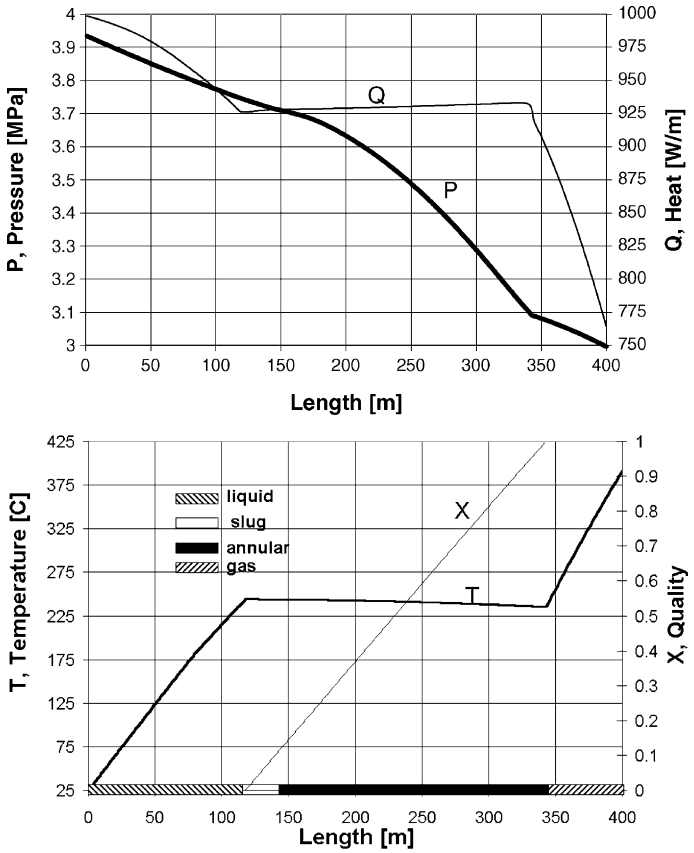

Fig. 5. Flow properties along the pipe, case 4. Flow pattern model with solar heating ($Q_{\text{im}} = 1000$ W/m, $W = 0.12$ kg/s, $\beta = 10°$).

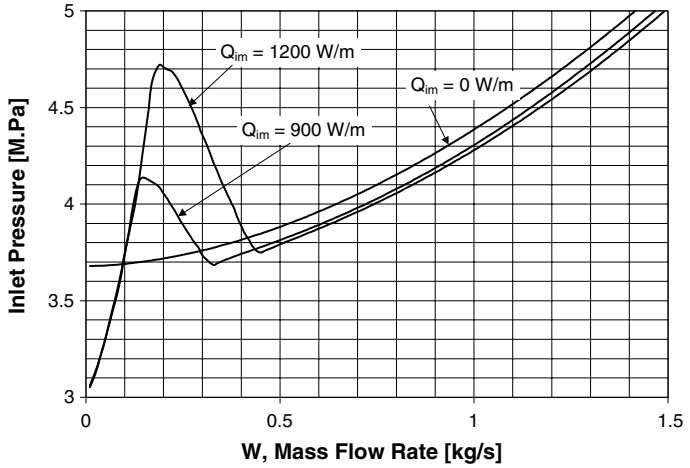

Fig. 6. Inlet pressure vs. mass flow rate, case 4, $\beta = 10°$.

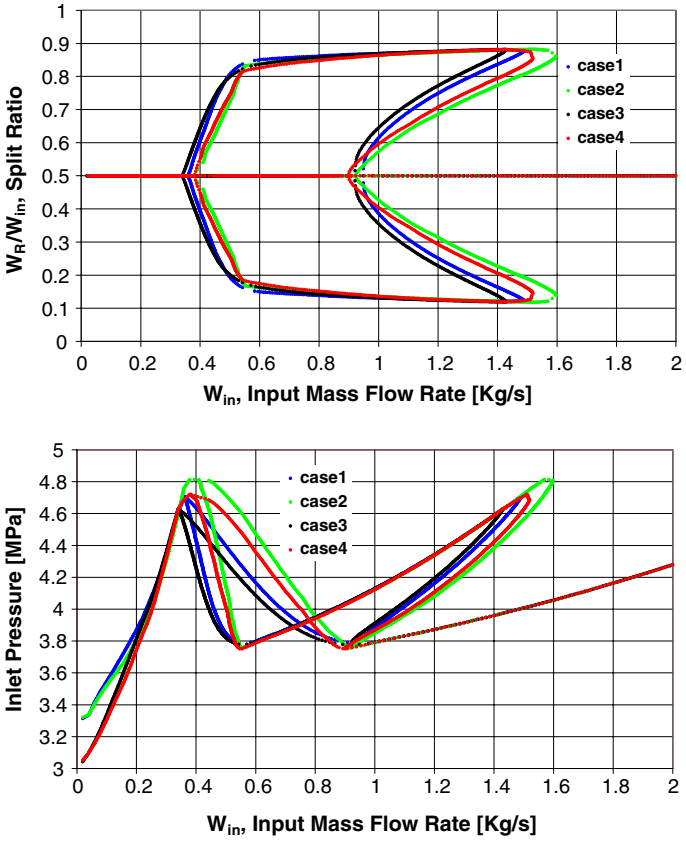

Fig. 7. Splitting ratio and inlet pressure for even heating, $\beta = 10°$. Right pipe—1200 (W/m), left pipe—1200 (W/m): case 1—drift flux model without heat losses to the surroundings; case 2—flow pattern without heat losses to the surroundings; case 3—drift flux with heat losses to the surroundings; case 4—flow pattern with heat losses to the surroundings.

Fig. 8 presents the effect of inclination for symmetric heating, for case 4. For low flow rates the splitting is symmetric and the fluid is mostly in the form of superheated steam in the pipe. In this region the effect of gravity is negligible and the effect of inclination on the pressure drop is minimal. For higher flow rate, the effect of inclination is quite pronounced.

In Figs. 9–11 the splitting ratios and the inlet pressures that are associated with the specific splitting ratios have the same line type. Thus one can identify the pressure drop solution with the corresponding solution for the splitting ratio.

Fig. 9 present the solutions of case 4 for even heating, $Q_{\mathrm{im,R}} = Q_{\mathrm{im,L}} = 1200$ W/m. The solid thick line is a solution for even splitting of the flow rate between the right and left pipes. The solid thick line at the bottom figure represents the corresponding inlet pressure for even splitting. For low and high flow rates even splitting is the only unique solution. However for intermediate flow rates we may have 3 or 5 solutions.

In the regions where multiple solutions exist the question is which one is the actual physical solution. Based on our previous experience for similar systems (Tshuva et al., 1999) we assume that the actual case in practice will be the solution that will result in a minimum pressure drop.

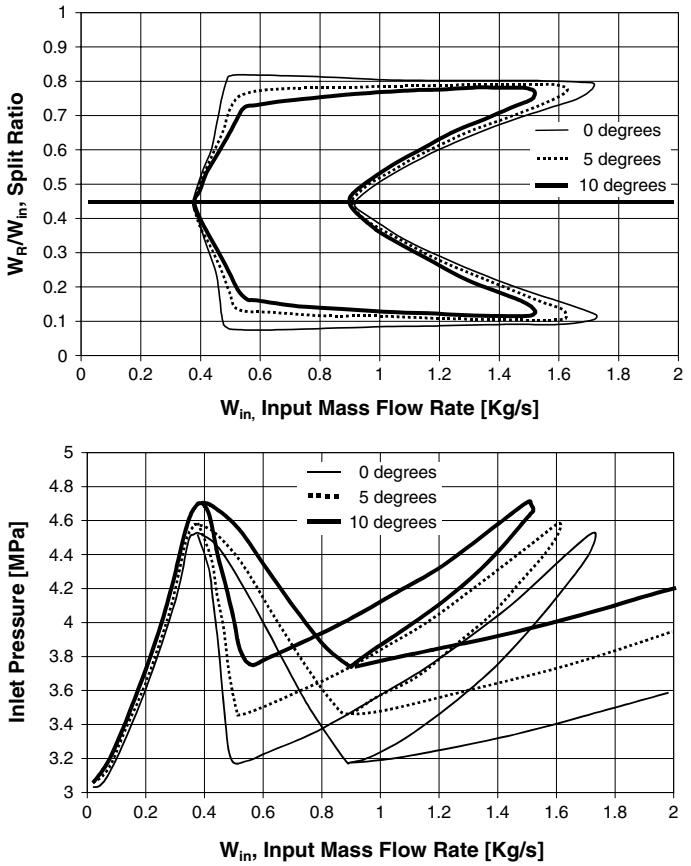

Fig. 8. Splitting ratio and inlet pressure for various inclinations angles, even heating. Case 4: right pipe—1200 (W/m); left pipe—1200 (W/m).

Fig. 9 shows that in the range of $W_{in} = 0.35$–0.75 the minimum pressure drop is associated with uneven splitting (the dotted line). Thus we would expect that for a given inlet flow rate the splitting in the aforementioned range will be uneven and may go down to 15% in one pipe and 85% in the other pipe. Outside of this range the flow is expected to be symmetric since the symmetric splitting is either the only solution or the solution that yields the minimum pressure drop (the solid thick line).

Fig. 10 shows the case of uneven heating, namely $Q_{im,R} = 1200$ W/m and $Q_{im,L} = 900$ W/m. Obviously in this case we do not have usually even splitting unless the flow rate is very high resulting in liquid flow in the two pipes without evaporation. Again for high and low flow rates the solution is unique. For intermediate flow rates we may have 3 or 5 solutions. Again, if we consider that the actual solution in practice will be the one with the minimal pressure drop we may observe quite a complex behavior. For low inlet flow rate, $W_{in} < 0.5$, one observe a single solution for the splitting ratio which decreases with increasing W_{in}. For $0.5 < W_{in} < 0.85$ we have three solutions for which the minimum pressure drop is presented first by the solid thick line, then by the dotted one followed by the solid thin line. For $W_{in} > 0.85$ one can observe five solutions, then three

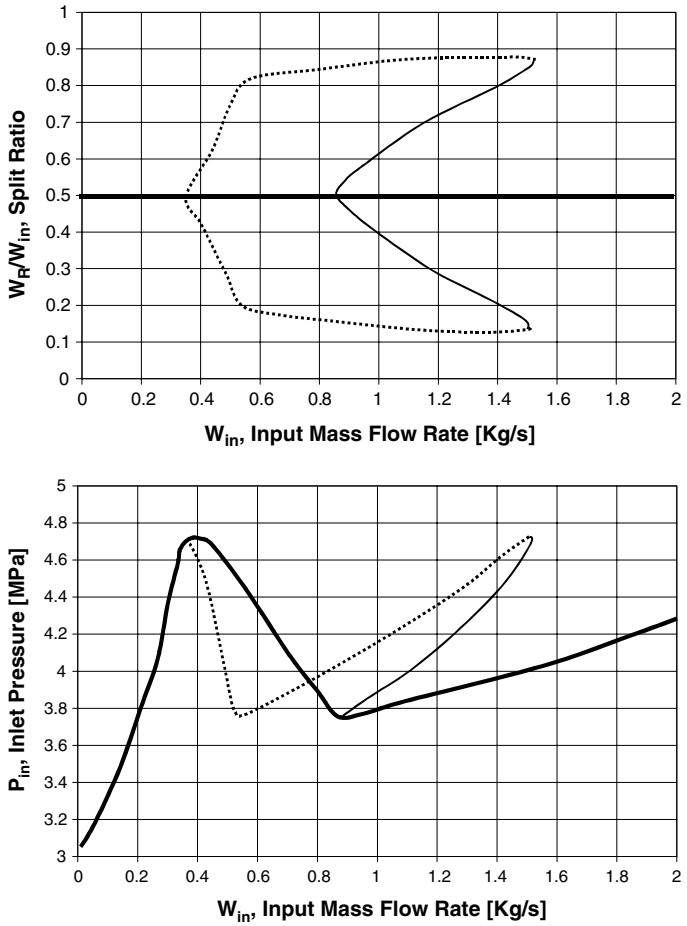

Fig. 9. Splitting ratio and inlet pressure for even heating, case 4, $\beta = 10°$. Right pipe—1200 (W/m), left pipe—1200 (W/m).

solutions and for high flow rate a single solution. In this region, however, the minimum pressure drop is presented by the dashdotted line, which is associated with even splitting.

Fig. 11 presents the case where no heating is applied to the left pipe. Up to $W_{\text{in}} = 0.7$ kg/s a single solution is obtained. In this region the fluid prefers to flow in the unheated pipe which is an unfavorable result from the practical point of view. For $0.7 < W_{\text{in}} < 1.4$ kg/s three steady state solutions are obtained for which the minimum pressure drop is presented by the solid thin line (approximately even splitting). For $W_{\text{in}} > 1.4$ kg/s a single solution, associated with even splitting is obtained.

The abovementioned results are related to a system with imposed inlet flow rate, W_{in}. The situation may be different for the case where an inlet pressure is imposed. In this case we expect Ledinegg (1954) instability along the curve that has a negative slop of the inlet pressure vs. the inlet flow rate. In this case the analysis of minimum pressure drop is expected to be valid only for the regions where the pressure drop has a positive slop with respect to the inlet flow rate.

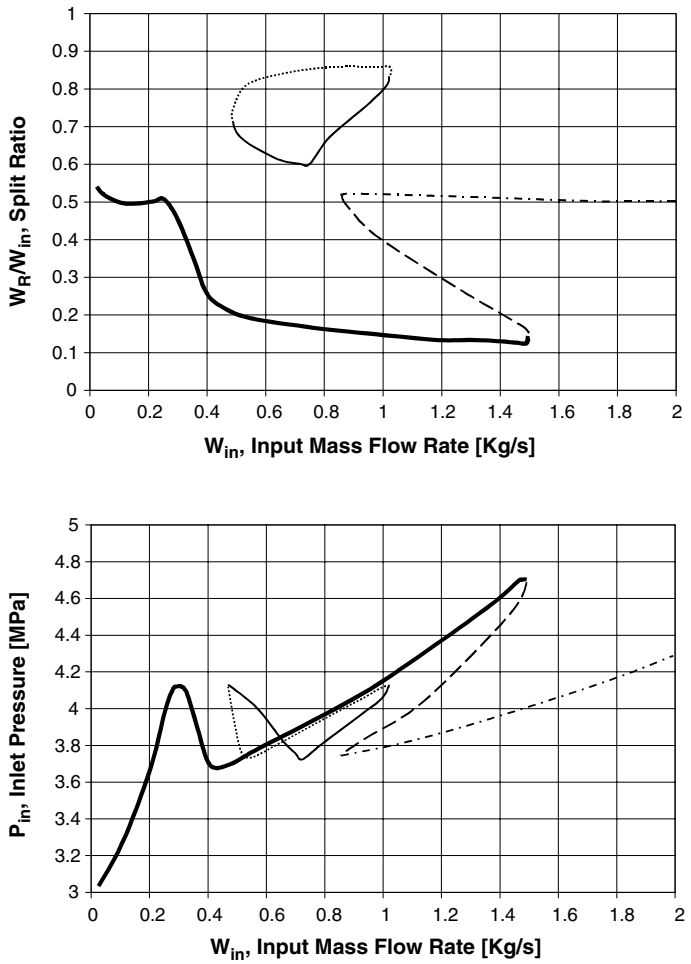

Fig. 10. Splitting ratio and inlet pressure for even heating, case 4, $\beta = 10°$. Right pipe—1200 (W/m), left pipe—900 (W/m).

4. Summary and conclusions

The splitting ratios for solar steam generation in two parallel pipes with a common inlet and outlet manifolds is calculated. The solution based on the drift flux model is a reasonable approximation for the calculation of the splitting ratios.

It is shown that the solution is not always unique and one can obtain 1, 3 or 5 solutions of the splitting ratios for each value of the inlet flow rate, W_{in}. It is speculated that the practical steady state solution is the one which yields the minimum pressure drop. Following this criteria one can observe discontinuities in the splitting ratio while changing the total inlet flow rate.

Splitting of the flow rate between the two parallel pipes, is not necessarily equal, even for symmetric heating. For the case of asymmetric heating most of the liquid tends to flow in the pipe which absorbs less heat than the other pipe. This is an unfavorable conclusion from the practical operational point of view.

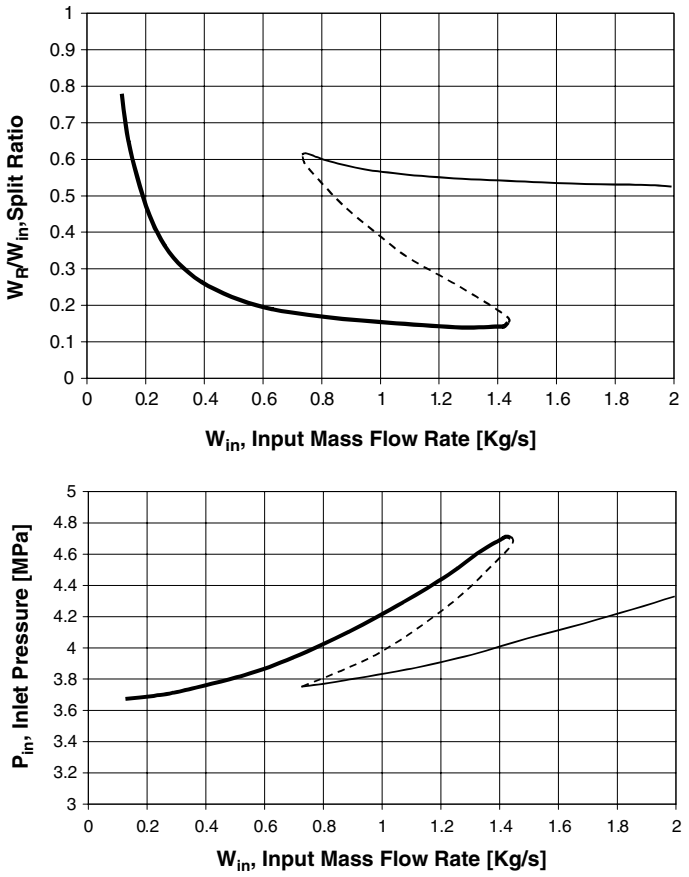

Fig. 11. Splitting ratio and inlet pressure for even heating, case 4, $\beta = 10°$. Right pipe—1200 (W/m), left pipe—0 (W/m).

References

Barnea, D., 1987. A unified model for prediction flow pattern transitions in the whole range of pipe inclination. Int. J. Multiphase Flow 13, 1–12.

Bendiksen, K.H., 1984. An experimental investigation of the motion of long bubbles in inclined tubes. Int. J. Multiphase Flow 10, 467–483.

Jovic, V., Afgan, N., Jovic, L., Spasojevic, D., 1994. An experimental study of the pressure drop oscillations in three parallel channel two-phase flow. In: 4th International Heat Transfer Conference, Brighton, UK, vol. 6, pp. 193–198.

Ledinegg, M., 1954. Instability of flow during natural and forced circulation. Die Waerme 61, AEC-TR-1861, pp. 891–898.

Nicklin, D.J., 1962. Two-phase bubble flow. Chem. Eng. Sci. 17, 693–702.

Ozawa, M., Akagawa, K., Sakaguchi, T., 1989. Flow instabilities in parallel-channel flow systems of gas–liquid two-phase mixtures. Int. J. Multiphase Flow 15, 639–657.

Ozawa, M., Akagawa, K., Sakaguchi, T., Suezawa, T., 1982. Oscillatory flow instabilities in a gas–liquid two-phase flow system. Heat Transfer in Nuclear Reactor Safety, Hemisphere, Washington, DC, pp. 379–390.

Ozawa, M., Akagawa, K., Sakaguchi, T., Tsukahara, T., Fujii, T., 1979. Oscillatory flow instabilities in air–water two-phase flow systems—1st report. Pressure drop oscillation. Bull. JSME 22, 1763–1770.

Reinecke, N., Griffith, P., Mewes, D., 1994. Flow-reversal in vertical, two-phase, two-component flow in parallel channels. In: 29th meeting of the European two-phase flow group, Siet, Piacenza, Italy.

Taitel, Y., Barnea, D., 1990. Two-phase slug flow. Adv. Heat Transfer 20, 83–132.

Taitel, Y., Dukler, A.E., 1976. A model for prediction flow regime transitions in horizontal and near horizontal gas–liquid flow. AIChE J. 22, 47–55.

Tshuva, M., Barnea, D., Taitel, Y., 1999. Two phase flow in inclined parallel pipes. Int. J. Multiphase Flow 25, 1491–1503.

Tong, L.S., 1975. Boiling Heat Transfer and Two-Phase Flow. Krieger Publishing Co.